Cellular and Molecular Life Sciences (2024) 81:362
https://doi.org/10.1007/s00018-024-05373-2

ORIGINAL ARTICLE

RXR nuclear receptor signaling modulates lipid metabolism and triggers lysosomal clearance of alpha-synuclein in neuronal models of synucleinopathy

Arati Tripathi[1] · Heba Alnakhala[1] · Lisa Brontesi[1] · Dennis Selkoe[1] · Ulf Dettmer[1]

Received: 29 March 2024 / Revised: 26 June 2024 / Accepted: 17 July 2024

Abstract

Disease-modifying strategies for Parkinson disease (PD), the most common synucleinopathy, represent a critical unmet medical need. Accumulation of the neuronal protein alpha-synuclein (αS) and abnormal lipid metabolism have each been implicated in PD pathogenesis. Here, we elucidate how retinoid-X-receptor (RXR) nuclear receptor signaling impacts these two aspects of PD pathogenesis. We find that activated RXR differentially regulates fatty acid desaturases, significantly reducing the transcript levels of the largely brain-specific desaturase SCD5 in human cultured neural cells and PD patient-derived neurons. This was associated with reduced perilipin-2 protein levels in patient neurons, reversal of αS-induced increases in lipid droplet (LD) size, and a reduction of triglyceride levels in human cultured cells. With regard to αS proteostasis, our study reveals that RXR agonism stimulates lysosomal clearance of αS. Our data support the involvement of Polo-like kinase 2 activity and αS S129 phosphorylation in mediating this benefit. The lowering of cellular αS levels was associated with reduced cytotoxicity. Compared to RXR activation, the RXR antagonist HX531 had the opposite effects on LD size, SCD, αS turnover, and cytotoxicity, all supporting pathway specificity. Together, our findings show that RXR-activating ligands can modulate fatty acid metabolism and αS turnover to confer benefit in cellular models of PD, including patient neurons. We offer a new paradigm to investigate nuclear receptor ligands as a promising strategy for PD and related synucleinopathies.

Keywords Parkinson's disease · Fatty acids · Alpha-synuclein · SNCA triplication · Nuclear receptor · Retinoid X Receptor agonist · Desaturases

Abbreviations

ALS	Amyotrophic lateral sclerosis
ALP	Autophagy lysosome pathway
AmCl	Ammonium chloride
DI	Desaturation index
DLB	Dementia with Lewy bodies
DMEM	Dulbecco's modified eagle medium
DMSO	Dimethyl sulfoxide
DIV	Days in vitro
FADS2	Fatty acid desaturase 2 or delta6-desaturase
FADS1	Fatty acid desaturase 2 or delta5-desaturase
FA	Fatty acid
FBS	Fetal bovine serum
fPD	Familial Parkinson's disease
GAPDH	Glyceraldehyde 3-phosphate dehydrogenase
GC-FID	Gas chromatography-flame ionization detection
GWAS	Genome-wide association study
LB	Lewy body
LD	Lipid droplet
LN	Lewy neurite
LAMP1	Lysosome-associated membrane glycoprotein 1
LC3	Microtubule-associated protein 1A/1B light chain 3
LDH	Lactate dehydrogenase
LDS	Lithium dodecyl sulfate
3-MA	3-Methyl adenine
mRNA	Messenger RNA

✉ Arati Tripathi
atripathi3@bwh.harvard.edu

✉ Dennis Selkoe
dselkoe@bwh.harvard.edu

✉ Ulf Dettmer
udettmer@bwh.harvard.edu

[1] Ann Romney Center for Neurologic Diseases, Brigham and Women's Hospital and Harvard Medical School, 60 Fenwood Rd, Boston, MA 02115, USA

Published online: 20 August 2024

MUFA	Monounsaturated fatty acid
NR	Nuclear receptor
PBS	Phosphate-buffered saline
PD	Parkinson's disease
PDD	Parkinson's disease dementia
PFA	Paraformaldehyde
Plk2	Polo-like kinase 2
pS129	Phospho-S129 αS
PUFA	Polyunsaturated fatty acid
PVDF	Polyvinylidene fluoride
qPCR	Quantitative polymerase chain reaction
RXR	Retinoid X receptor
SCD	Stearoyl-CoA desaturase
SNCA	Alpha-synuclein
TBS	Tris-buffered saline
TG	Triglycerides
UPS	Ubiquitin proteasome system
WB	Western blot

Introduction

The accumulation of proteinaceous inclusions in the brain is a common feature among neurodegenerative diseases. Alpha-synuclein (αS)-rich inclusions in neuronal somata (Lewy body, LB) and neurites (Lewy neurite, LN) are the defining neuropathological hallmarks of neurodegenerative diseases [1] collectively called synucleinopathies. These diseases include Parkinson's disease (PD), PD dementia (PDD), and dementia with Lewy bodies (DLB). Of the synucleinopathies, PD is the most prevalent, affecting nearly 10 million people worldwide [2]. PD is characterized by bradykinesia, rigidity, postural instability, and tremor as well as non-motor symptoms, all of which worsen over time [3]. Current treatments for PD are aimed at symptom management. No approved therapies exist to cure, slow, or halt this debilitating disease. Therapeutic strategies thus represent a critical unmet medical need.

The disease-associated protein αS, encoded by the *SNCA* gene, is a conserved, 14 kilo-Dalton synaptic protein linked to both familial (fPD) and sporadic PD. While the underlying causes of sporadic PD remain largely unknown, the *SNCA* gene locus has shown the strongest signal in genome-wide association studies (GWAS) [4] and has also been found as a modifier of age at onset of sporadic PD [5, 6]. Moreover, *SNCA* was the first mutant gene (A53T) identified to cause autosomal dominant PD [7] and, since then, several other missense mutations—A30P [8], E46K [9], H50Q [10], G51D [11, 12], A53E [13], A53V [14], and A30G [15]—have each been identified as causative of fPD. Importantly, genomic duplication and triplication of the *SNCA* locus lead to life-long increase in wild-type (WT) αS levels, causing aggressive, early-onset forms of fPD [16–20]. Indeed, age at motor symptom onset and rate of motor progression to death correlate with the level of *SNCA* expression [5]. In accord, some early-onset sporadic PD patients have been identified to have increased αS burden despite absence of known PD-associated monogenic mutations or extra copies of *SNCA* [21].

While the abundant neuronal protein αS has thus been firmly linked to neuronal loss in the brains of PD patients, its exact role in PD pathogenesis remains poorly understood. Diverse mechanisms including proteotoxicity, disturbed vesicle trafficking, mitochondrial dysfunction, and dysregulated protein clearance have all been suggested [22, 23]. Emerging evidence implicates perturbed lipid balance and metabolism as important factors in the disease [24–26]. Accordingly, in addition to their αS accumulation, LBs have been reported to be enriched in lipids and membranous organelles [27–30]. αS itself has physiologic and pathogenic interactions with membrane phospholipids [31–34] and with fatty acids (FAs) [35, 36], and it can alter lipid homeostasis [37]. Overexpression of αS promotes lipid droplet (LD) formation [38–40], and changes in LD content and distribution have been associated with αS toxicity, neurodegeneration, and altered membrane trafficking [24–26], indicating an intimate connection between αS expression and FA homeostasis. Supporting this notion, LD accumulation has been identified by histology of neurons in PD patient brains [41]. Collectively, these observations suggest that modulating PD-relevant lipid phenotypes could serve as a useful strategy for αS-directed therapeutic intervention.

Nuclear Receptors (NRs) are transcription factors that have the ability to perceive extracellular cues as well as altered intracellular environments to initiate downstream homeostatic responses. Indeed, activated NRs can modulate a diverse array of pathways affecting cell proliferation, development, mitochondrial function, and FA metabolism through targeted genes [42–44]. Given their important role in physiology and their ability to respond to small lipophilic ligands, NRs have emerged as valuable therapeutic targets and generated interest in neurodegenerative diseases in the past decade [43, 45]. To function, non-steroidal ligand-activated NRs require retinoid-X-receptor (RXR) as a heterodimerization partner [42, 44, 46, 47]. Indeed, small-molecule drugs have been explored as activators of RXR signaling and were shown to impart neuroprotective effects associated with improved memory and cognition in models of certain neurologic diseases including Alzheimer's and Huntington's disease [48–52]. In toxin-based cellular and murine models of PD, RXR ligands have provided promising results in neuroprotection [53–55]. Despite these observations, the impact of activating RXR on αS-based models of PD, and any direct or indirect effect on αS, have largely remained unexplored.

Here, we systematically examined both RXR agonism and antagonism using pharmacological modulators to explore how RXR signaling influences PD-relevant phenotypes in cellular models. In particular, we focused on FA metabolism and αS proteostasis, both strongly implicated in PD pathobiology. Our results show that pharmacological activation of RXR using multiple small-molecule agonists (LG1069/bexarotene, LG754 and HX630) ameliorates cytotoxicity in M17D human neural cells expressing αS. Mechanistically, our data indicate that RXR agonism differentially regulates FA desaturases, namely stearoyl-CoA desaturase (SCD1 vs. SCD5) and delta6-desaturase (FADS2). In both αS-expressing human M17D cells and αS triplication PD patient-derived neurons, SCD5 transcript levels were significantly reduced upon RXR agonism. Further, we found that pharmacological activators of RXR limit αS-induced increases in LD size, reduce levels of the LD-associated protein perilipin-2, and mediate reduction of triglycerides in αS-expressing human M17D cells. We discovered that RXR activation triggers clearance of αS via lysosomal pathways. Our data suggest the involvement of Polo-like kinase (Plk2) activity vis-à-vis αS serine-129 phosphorylation in mediating this clearance. The effects of RXR activation on LD size, SCD, αS turnover, and cytotoxicity were reversed by the RXR antagonist HX531, showing pathway specificity. These multifaceted results indicate that RXR-activating ligands can ameliorate PD-relevant phenotypes in cellular models of synucleinopathy and offer a new direction to explore NR ligands as potential therapeutics for PD and DLB.

Materials and methods

Antibodies. Human αS (mouse, Thermo Fisher 4B12; rat, Enzo Life Sciences 15G7), human pS129 αS (rabbit, Cell Signaling Technology D1R1R; rabbit Abcam MJFR13), GAPDH (mouse, Abcam 6C5), LC3B (rabbit, Cell Signaling Technology #2775), p62 (Cell Signaling Technology #5114), β3-tubulin (Abcam #18,207), LAMP1 (Abcam #25,245), SCD1 (Abcam #236,868) and 4-hydorxynonenal (Millipore Sigma #5605). The two bands immunoreactive to SCD1 antibody are specific for SCD1 and absent in knock-out cell lysates as per manufacturer (Abcam). Secondary antibodies were anti-rabbit Fluorescent LiCor IRDye 800CW, anti-mouse Fluorescent LiCor IRDye 680RD, anti-rat Fluorescent LiCor IRDye 680RD.

Cell Lines, cell culture, transfections. Tet-on M17D-TR/αS::YFP [56] and M17D/αS stably transduced cells [57] have been described before and were cultured at 37 °C in a 5% CO_2 atmosphere in Dulbecco's modified Eagle's medium (DMEM) supplemented with 10% FBS and 2 mM Glutamine supplement (Gibco). Lipofectamine 2000 (Invitrogen) was used for transient transfection according to the manufacturer's instructions.

iPSC neuron culture. The *SNCA* triplication iPSC line was obtained from The European Bank for induced pluripotent Stem Cells (EBiSC) (#EDi0001-A) along with the isogenic CRISPR-corrected control line (#EDi0001-A4), in which the start codon of two copies of the SNCA gene had been disrupted by CRISPR/Cas [18, 58]. Each line was transduced with TetO-Ngn2-Puro to establish "NR" (neurogenin-2 + rtTA) iPSCs. Neurogenin-2-mediated differentiation was achieved with minor modification to previous protocols [59, 60]. All neurons were grown on Matrigel (Corning Life Sciences) coated plates and used for experiments between DIV17-21. Medium was replaced completely on DIV5 (Neurobasal medium supplemented with B-27, BDNF/GDNF/CNTF/Dox/Puromycin), and 50% on DIV8 (same media as DIV5), DIV12 (same media as DIV5 except no Dox and Puromycin) and DIV16 (same as DIV12). Drugs/vehicle were added for 72 h.

Immunoblotting. M17D cells: Cells were lysed in 1X LDS buffer (NuPAGE, Thermo Fisher Scientific). Triplication neurons: a modified RIPA buffer (RIPA + 1% Triton X-100) supplemented with protease and phosphatase inhibitors Halt Protease inhibitor cocktail, Thermo Fisher Scientific) was used. LDS sample buffer was added to 1X final concentration. All samples were boiled for 10 min at 98 °C and run on NuPAGE 4–12% Bis–Tris gels (Invitrogen). Transfers onto either nitrocellulose or PVDF membranes were performed using program P0 on an iBlot 2 (Invitrogen). For experiments involving αS detection, membranes were first fixed for 10 min in 4% PFA (in PBS). Membranes were washed 2x with DI water for 5 min and blocked using PBS Intercept Blocking buffer (LI-COR) for 45 min at room temperature. Membranes were incubated in primary antibody in Blocking buffer overnight at 4 °C. For experiments involving measurement of pS129, blocking was done in TBS Intercept Blocking Buffer (LI-COR), and primary antibodies diluted in TBS Blocking Buffer. For LC3, p62, nitrocellulose membranes were used, and blocking and primary antibody incubation done in 3% BSA/PBS solution. All membranes were washed 3x in PBS or TBS with 0.1% Tween-20 and incubated in appropriate secondary antibodies (LI-COR). Membranes were imaged on an Odyssey CLx scanner (LI-COR).

Lactate dehydrogenase (LDH) release assay. 4000 cells/well were plated in a 96-well plate (Corning) and allowed to adhere for 24 h. They were treated for 2 h with vehicle (DMSO) or drugs at concentrations indicated in figure legends before αS::YFP expression was induced with Dox addition. 72 h post-induction, 80 µL medium were collected and used in an LDH release assay (CytoTox 96® Non-Radioactive Cytotoxicity Assay, Promega) following the manufacturer's instructions. αS triplication neurons were

treated with vehicle (DMSO) or drugs on DIV17 for 72 h. 100 µl medium were collected for LDH release assay.

Live-cell imaging and quantification. Live cell imaging was performed on an Incucyte Zoom machine (Essen Biosciences). Lipid droplet dye: Same experimental set-up as LDH assay except at 72 h, Lipidspot^{610} dye (Biotium) was added and cells incubated with dye for 2 h. Fluorescence signals were determined to estimate LD size, number and total integrated intensity quantified using Incucyte software with the following processing definition: Adaptive background subtraction, threshold (GCU) 1.2; edge split on, sensitivity 73; cleanup: hole fill 5 µm^2; filters: eccentricity min 0.2, mean intensity min 2. Lysotracker Red: Same experimental set-up as LDH assay except at 72 h, Lysotracker™ Deep red (Thermo Fisher Scientific) was added. Cells were incubated for 1 h and Lysotracker fluorescence was quantified using the Incucyte software with the following processing definition: Top hat background subtraction, radius 10 µm, threshold (GCU) 0.2; edge split on, sensitivity -8; filters: eccentricity min 140.

Immunofluorescence. αS triplication neurons were seeded at 7000 cells/well of a Matrigel-coated 96-well plate. Vehicle or drug treatment was performed as described under iPSC neuron culture. Cells were fixed with 4% paraformaldehyde in 20% sucrose, permeabilized and blocked in TBS containing 0.1% Triton and 5% goat serum. Samples were incubated with primary antibodies (LAMP1, β3-tubulin) in the same solution overnight at 4 °C, washed with TBS, followed by incubation with appropriate Alexa Fluor secondary antibodies. After a second round of washes, Hoechst dye (Thermo Fisher Scientific) was added for 5 min at room temperature and cells were washed again to remove excess dye. Images were acquired using InCell Analyzer (GE Healthcare) at 40X. Nuclei were defined and LAMP1 signal intensity computed using ImageJ. 40 neurons were analyzed for DMSO and drug treatment, analyst was blinded to the image category. DAPI positive neurons were segmented using "Triangle" threshold algorithms, ImageJ. The LAMP1 signal intensity was measured via DAPI ROIs (Regions of Interest).

Lysosome inhibition. Identical experimental set-up as LDH assay, except at 96 h cells were treated with LG1069 and either 3-MA (10 mM) or Ammonium Chloride (AmCl, 30 mM) for 4–6 h, followed by cell lysis and subsequent immunoblotting.

Triglyceride extraction. Triglyceride extraction and quantification from cell lysates was carried out with the Triglyceride Assay Kit (Abcam, #65,336) as per manufacturer's instructions. Colorimetric measurements were done on a SpectraMax Plus 384 Microplate Reader (Molecular Devices LLC).

RNA extraction, reverse transcription, and q-PCR. αS::YFP: 300,000 cells/well of a 6-well plate (Corning) were plated and allowed to adhere for 24 h. αS::YFP expression was induced for 72 h, followed by treatment for 48 h with vehicle (DMSO) or 2 µM LG1069. Cells were pelleted, washed and frozen at − 20 °C till further use. iPSC neurons: 250,000 DIV4 neurons/well of Matrigel-coated 24-well plate were used. Treatment paradigm was as described in the "iPSC neuron culture" section above. RNA extraction was performed with mirVana™ miRNA Isolation Kit, without phenol (Thermo Fisher Scientific #AM1561) as per manufacturer's instructions. RNA purity was then assessed through High Sensitivity RNA Screen Tape assay in 2200 TapeStation system (Agilent) and RNA concentrations were determined by Nanodrop. cDNA was synthesized with SuperScript IV VILO Master Mix (Invitrogen, #11756050) in a Thermal cycler (BIORAD). TaqMan RT qPCR was performed using probes for SCD1 (Thermo Fisher Scientific Hs01682761_m1, #4331182), SCD5 (Thermo Fisher Scientific Hs00227692_m1, #4331182), SNCA (Thermo Fisher Scientific Hs00240906_m1 #4331182), and Beta-2-Microglobulin (B2M) (Thermo Fisher Scientific Hs00187842_m1, #4331182). The reaction was run on a QuantStudio Flex 7 qPCR system and the delta-delta threshold cycle (ΔΔCt) calculations were made using QuantStudio software (ThermoFisher Scientific).

Lipidomics. 1.5 million cells were plated in a 10 cm dish (Corning) and allowed to adhere for 24 h. They were induced for αS::YFP expression for 72 h and treated for 48 h with vehicle (DMSO) or 2 µM LG1069. Uninduced, untreated cells were used for baseline readings and grown in parallel to treated cells. Cells were pelleted and counted. Equal numbers of cells were collected for each condition, washed with PBS, and stored at − 80 °C until shipment to OmegaQuant (Sioux Falls, SD). Phospholipid FA composition was analyzed at OmegaQuant by gas chromatography with flame ionization detection. Desaturation indices (DI) were computed as ratio of product to substrate FAs for FADS2 (C18:3n6 to C18:2n6 ratio), FADS1 (C20:4n6 to C20:3n6 ratio) and SCD (C16:1n7 to C16:0, C18:1n9 to C18:0 ratios). DI values computed for induced cells and induced/treated cells were normalized to uninduced, untreated cells.

Statistical analyses. Statistical analyses were performed by t-test (2 groups) with or without Welch's correction or one-way ANOVA (> 2 groups) with Sidak's or Dunnett's multiple comparison post hoc test. For non-parametric tests, Kolmogorov–Smirnov test was performed. Grubbs method (0.05) was used to identify outliers. Only one data point was identified by this method and removed (Fig. 3A(FADS2)).. The number of independent experiments (N) and p-value for criteria of significance are described in the figure legends. Values in graphs are mean ± SD. All statistical analyses were done using GraphPad Prism version 10 following the program's guidelines.

Results

Pharmacological activation of RXR nuclear receptors improves cellular health of αS-expressing human neural cells

To search for an interplay between RXR activity and αS in cellular models of PD, we took advantage of our previously reported [56] human M17D neural cells that, in the presence of doxycycline (Dox), express YFP-tagged WT αS (Fig. 1A). Our lab as well as other groups have utilized human M17D cultured cells for therapeutic discovery and validation [37, 56, 57]. The well-characterized small-molecule RXR agonist LG1069 (Fig. 1B, left), also known as bexarotene, is an FDA-approved potent RXR agonist currently used for treatment of cutaneous T-cell lymphoma [61]. Beneficial effects of this small-molecule RXR-agonist have also been reported in neurodegenerative models of Alzheimer's disease, Huntington's disease, ALS, and a 6-OHDA toxin-based model of PD [48, 51–53]. However, its potential benefits in αS-based models of synucleinopathy and effects on αS itself have been unaddressed. To assess if LG1069 can ameliorate αS-related cytotoxicity, human M17D cells were induced to express WT αS::YFP in the presence or absence of LG1069, and lactate dehydrogenase (LDH) release was measured as a proxy for compromised cell health. αS::YFP expression

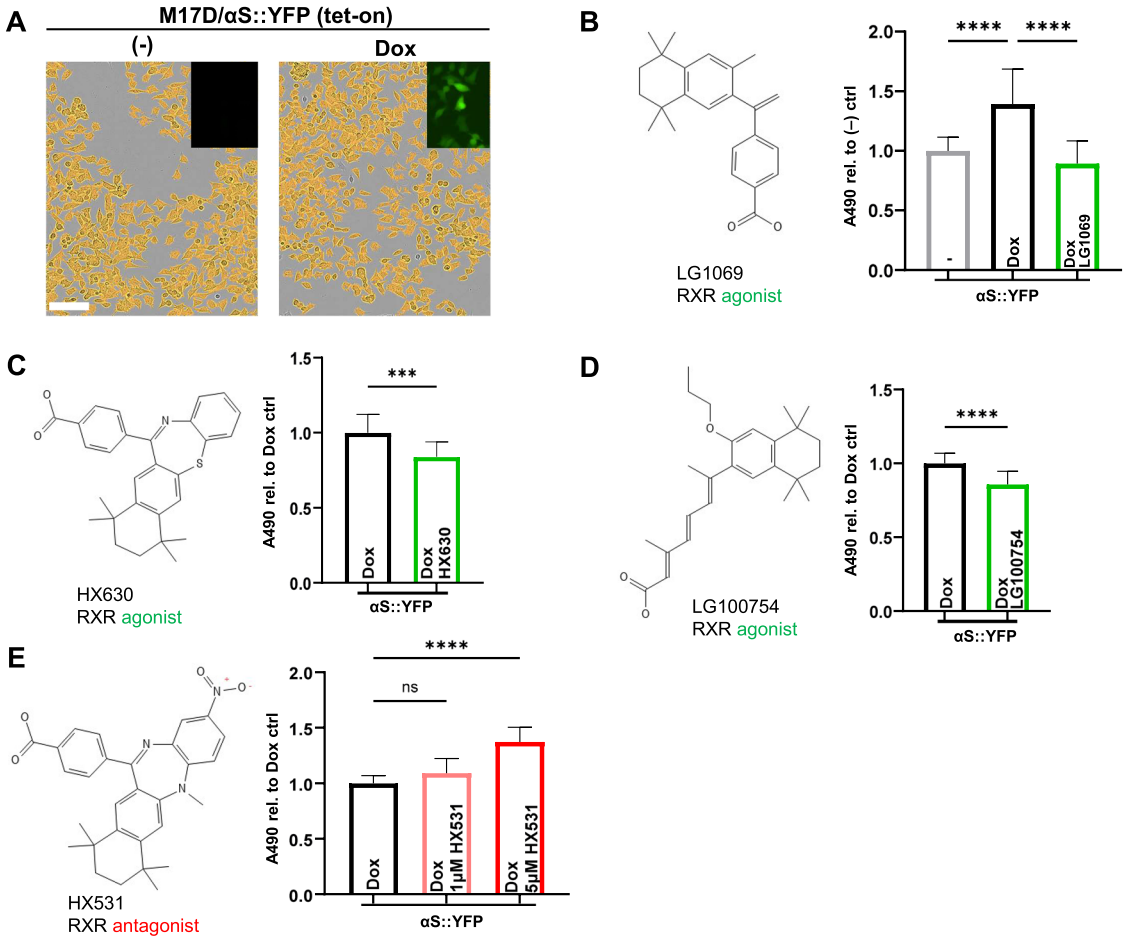

Fig. 1 Effect of pharmacological RXR modulators on αS-expressing M17D human neural cells. **A** Left, uninduced control (–) cells. Right, doxycycline (Dox) induction of 'tet-on' WT αS::YFP expression in M17D cells. Bright-field (cells identified by Incucyte live-cell microscopy shown in orange) and YFP fluorescence images (inset) at $t = 72$ h. Scale bar, 100 µm. **B** Left, chemical structure of RXR agonist LG1069. Right, cytotoxicity measured by lactate dehydrogenase (LDH) release assay in uninduced (–) vs. induced plus DMSO vehicle-treated (Dox) vs. induced plus 1 µM LG1069-treated cells. αS::YFP induction for 72 h post-treatment. Final readout of the LDH assays was absorbance at 490 nm, plotted relative to uninduced cells (–). N = 4. **C** Chemical structure of RXR agonist HX630 and LDH release assay analogous to B, but 1 µM HX630 was applied. Quantitation relative to induced vehicle-treated cells (Dox). N = 3. **D** Chemical structure of RXR agonist LG100754. LDH release assay analogous to C, but 1 µM LG100754 was applied. N = 4. **E** Chemical structure of RXR antagonist HX531 and LDH release assay analogous to **C** and **D**, but 1 µM and 5 µM HX531 were used. N = 3. All data are mean ± SD. *ns* not significant, ***$p < 0.001$, ****$p < 0.0001$

markedly increased LDH release into the medium relative to uninduced cells, consistent with αS-related toxicity (Fig. 1B, right). Addition of LG1069 attenuated LDH release, indicating an improvement in cell viability and reversal of αS toxicity (Fig. 1B, right). Next, we tested additional pharmacological RXR agonists, HX630 [62] and LG754 [63] in the LDH release assay. Treatment with HX630 (Fig. 1C, Left) or LG754 (Fig. 1D, top panel) were similarly associated with decreased LDH release and thus improved cell viability (Fig. 1C, D). We reasoned that if these beneficial effects were via RXR signaling, an RXR-selective antagonist, HX531 [64] (Fig. 1E, Left), would impact cellular health negatively. To test this hypothesis, cells were treated with vehicle (DMSO) or increasing concentrations of HX531 (Fig. 1E) and LDH release was assayed. Indeed, an elevation in LDH release was observed upon treatment with 5 µM HX531 relative to control cells (Fig. 1D). The use of pharmacological modulators, both agonists and an antagonist, collectively demonstrate that signaling via RXR can alter the viability of αS-expressing human neural cells and that small-molecule agonists of RXR activity can mitigate αS-mediated impaired health of these cells.

Pharmacological activation of RXR in αS-expressing human neural cells reduces lipid droplet size and decreases triglycerides

NRs are known to modulate cellular lipid metabolism through targeted gene regulation [44, 65]. Lipids play an important role in a number of cellular pathways associated with PD such as oxidative stress, endosomal-lysosomal pathway dysfunction, ER stress, and altered immune responses. Indeed, several genes involved in lipid metabolism have been identified in GWAS as risk factors for PD [66]. Lipidomic studies have also reported PD-related lipid alterations in both patient brains and plasma [25, 26, 67]. LDs are a central hub for FA storage and metabolism in cells [68, 69]. They consist of a core of neutral lipids, predominantly triacylglycerols (TGs) and sterol esters, surrounded by a monolayer of phospholipids. Accumulation of LDs within dopaminergic neurons of PD patient brains has recently been reported [41], implicating their relevance to PD. Given that NRs modulate lipid pathways, and alterations in these pathways are associated with PD, we asked whether pharmacological activation of the RXR might impact LDs. We treated M17D cells expressing αS::YFP with the RXR agonist LG1069 and visualized LDs with a neutral lipid dye (Lipidspot, Biotium) by Incucyte live-cell imaging. Automated software was subsequently used to quantify different parameters of LDs such as count, size, and total integrated intensity (Fig. 2A). Compared with uninduced cells, αS::YFP expression led to an increase in size, number, and thus total integrated intensity of LDs (Fig. 2A). As a control, the addition of Dox to parental M17D cells did not affect LDs (Supplementary Fig. 1). This indicated an αS-dependent effect, which is consistent with studies in multiple model systems such as yeast cells, *Drosophila,* and rodent neurons showing an elevation of LDs upon αS expression (37–39). Next, treatment of αS::YFP-expressing cells with LG1069 led to a reduction in LD size while LD number was unchanged (or only slightly reduced), resulting in decreased LD integrated intensity (Fig. 2A). To confirm this effect, we used another RXR-agonist (HX630) in the same experimental paradigm. HX630-treated cells exhibited a reduction in LD size (Fig. 2B). In contrast, treatment with RXR antagonist HX531 markedly increased LD size (Fig. 2C).

LDs are ubiquitous organelles that serve as intracellular stores by compartmentalizing lipids, mainly in the form of TGs. We hypothesized that the smaller LDs observed upon LG1069 treatment could therefore reflect a reduction in cellular TG accumulation. To test this hypothesis, we extracted total TGs from αS::YFP-expressing human M17D cells in the absence or presence of LG1069. Relative to untreated cells, we observed a reduction in total cellular TGs upon LG1069 treatment (Fig. 2D). Taken together, our results suggest that RXR activation alters FA metabolism, decreasing TG levels and thus LD size.

RXR modulation impacts FA desaturases differentially

Targeted regulation of FA desaturases by NR ligands [70–72] can lead to alterations in cellular lipid metabolism. We, therefore, asked whether RXR agonism impacts the activity of FA desaturases in our neuronal models. We chose to focus on the key desaturases in humans, Delta5-desaturase (D5D, also known as FADS1), Delta6-desaturase (D6D or FADS2), and stearoyl-CoA desaturase (SCD, also D9D), with D6D/FADS2 and SCD being implicated in TG/LD metabolism [56, 73, 74]. These enzymes catalyze the biosynthesis of monounsaturated FAs (MUFAs) in the case of SCD and polyunsaturated FAs (PUFAs) in the case of D5D and D6D by introducing double-bonds in the fatty acyl chain. To assess the impact of RXR agonism on FA desaturase activity, we administered LG1069 or vehicle to αS::YFP-expressing M17D cells. Untreated, uninduced cells were considered as the baseline control (indicated as a grey dashed line in Fig. 3A). Lipids were extracted under all three conditions (from uninduced/untreated cells, from αS-induced only cells and from αS-induced/LG1069-treated cells), hydrolyzed to individual fatty acyl chains, derivatized as FA methyl esters, and quantified by gas chromatography with flame ionization detection (GC-FID, OmegaQuant, Sioux Falls, SD). This approach provided an unbiased estimate of the ratio of the PUFAs gamma-linolenic acid

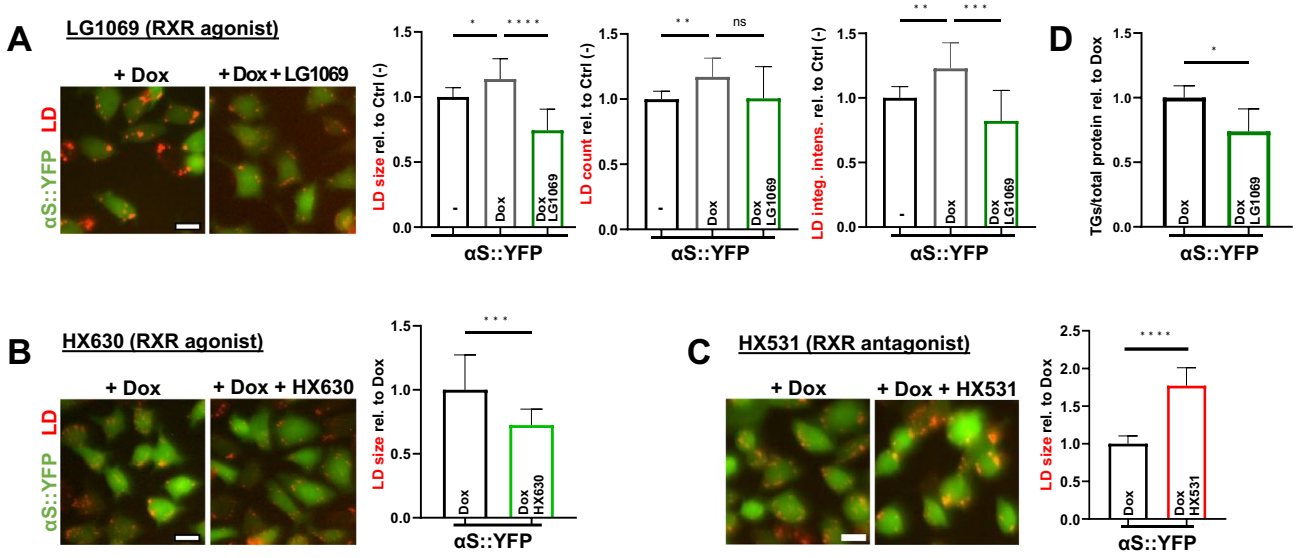

Fig. 2 RXR activation reduces lipid droplet size and triglycerides in αS-expressing human neural cells. **A** Left, induced tet-on M17D/αS::YFP cells were treated with DMSO vehicle or RXR activator LG1069 (1 µM). Incucyte live-cell microscopy (green: αS::YFP, red: lipid droplets = LDs visualized by Lipidspot[610]. Middle left, Incucyte-based quantification of LD size relative to uninduced untreated cells (−). Middle right, quantification of LD count. Right, quantification of LD integrated intensity. N = 4. **B** Analogous to A, but RXR activator HX630 (1 µM) was applied. Quantitation of LD size relative to induced vehicle-treated cells (Dox). N = 3. **C** Analogous to A, but RXR antagonist HX531 (5 µM) was applied. Quantitation of LD size relative to induced vehicle-treated cells (Dox). N = 3. **D** Induced M17D/αS::YFP cells treated with vehicle or RXR activator LG1069 (2 µM). Triglyceride (TG)/total protein quantification relative to vehicle control. N = 3. All data are mean ± SD. *ns* not significant, *$p < 0.05$. **$p < 0.01$. ***$p < 0.001$. ****$p < 0.0001$. Scale bars, 20 µm

(18:3n-6) to linoleic acid (18:2n-6), which is related to D6D desaturase activity (Fig. 3A, left graph). Conversion of dihomo-γ-linolenic acid (20:3n-6) to arachidonic acid (20:4n-6) served as an indicator of D5D desaturase activity (Fig. 3A, middle left graph). Lastly, the desaturation index (DI; mono-unsaturated to saturated FA ratio) for FAs of 16 carbons (C16:0, palmitic acid; C16:1n7, palmitoleic acid; Fig. 3A, middle right graph) or 18 carbons (C18:0, stearic acid, C18:1n9, oleic acid; Fig. 3A, right graph) as a measure of SCD activity. Interestingly, induced expression of αS::YFP led to a pronounced increase in D6D activity and a smaller rise in SCD C16DI activity, with little effect on D5D activity and or SCD C18DI activity (Fig. 3A). Treatment with LG1069 resulted in significant reduction of D6D activity, a modest decrease in D5D activity, and a subtle augmentation in SCD C16DI and C18DI (Fig. 3A).

To better understand the distinct and contrasting effects of LG1069 on LDs, TGs and SCD desaturation index, we chose to consider both SCD1 (ubiquitously expressed) and SCD5 (brain-specific expression), the two human isoforms of SCD [74, 75]. We first asked whether the subtle increase in SCD activity in response to LG1069 (Fig. 3A) correlated with the expression of one or both SCD isoforms. WB analysis of LG1069-treated vs. untreated cells suggested that LG1069 modestly increases SCD1 protein levels (Fig. 3B). Conversely, treatment with the RXR antagonist HX531 decreased SCD1 levels in a dose-dependent manner (Fig. 3C). Because we were unable to validate commercially available SCD5-specific antibodies, we quantified the brain-specific SCD5 enzyme (alongside SCD1) at the mRNA level by quantitative PCR (qPCR) (Fig. 3F). Consistent with protein levels, LG1069 also increased SCD1 mRNA (Fig. 3F). In sharp contrast, SCD5 transcripts were substantially reduced upon LG1069 treatment (Fig. 3F).

We next analyzed αS/FA interplay in response to RXR-activation in PD patient-derived αS triplication iPSC neurons as a cellular model of humans with PD. Increased levels of αS via triplication of the endogenous αS locus causes early-onset, severe PD [16]. To test whether RXR agonism alters SCD1 protein levels similar to our observation in human M17D cells, αS triplication and isogenic control neurons were treated with either vehicle or LG1069. WB quantification revealed an LG1069-dependent increase in SCD1 levels in αS triplication, but not in isogenic control neurons (Fig. 3D). Conversely, RXR antagonism via HX531 led to a reduction of SCD1 levels in the triplication neurons (Fig. 3E), signifying RXR pathway specificity. We next asked how SCD5 transcript levels respond to RXR agonism in the triplication neurons: similar to our observation in human M17D cells, LG1069 agonist treatment induced a decrease in SCD5 transcripts (Fig. 3G). RXR activation with

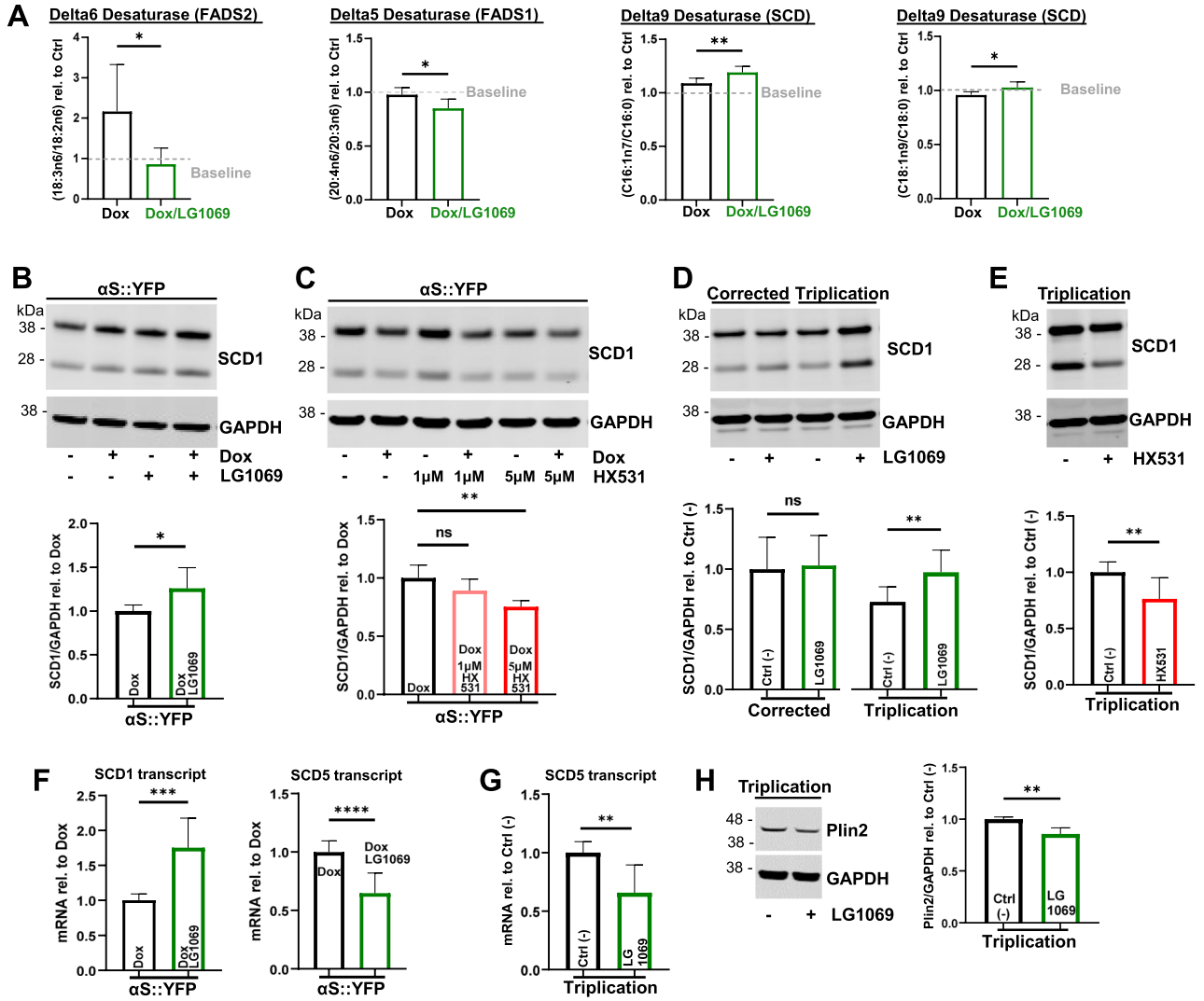

Fig. 3 Activated RXR signaling impacts cellular fatty acid desaturases differentially. **A** Fatty acid desaturase activities based on desaturation indices (DI) in induced/vehicle (Dox) vs. induced/LG1069 (Dox, LG1069) human M17D/αS::YFP cells (baseline: uninduced untreated cells set to 1). From left to right: Delta6 desaturase (FADS2) DI (C18:3n6 to C18:2n6 ratio), Delta5 desaturase (FADS1) DI (C20:4n6 to C20:3n6 ratio), Delta9 desaturase (SCD) DI (C16:1n7 to C16:0, C18:1n9 to C18:0 ratios). N = 2. **B** Top, WB analysis of SCD1 levels in uninduced and induced M17D/αS::YFP cells, treated with vehicle DMSO or RXR agonist LG1069 (1 μM); loading control: GAPDH. Bottom, quantification of SCD1/GAPDH ratios in induced/LG1069 (Dox, LG1069) cells relative to induced/vehicle treated cells (Dox, set to 1). N = 3. **C** Analogous to (**B**), but RXR antagonist HX531 (1 μM and 5 μM) was used. N = 3. **D** Top, WB analysis of SCD1 levels in PD patient-derived αS triplication iPSC neurons and isogenic control (Corrected), vehicle- vs. LG1069-treated (1 μM). Bottom, quantification of SCD1/GAPDH ratios relative to the respective vehicle control (–; set to 1). N = 3. **E** Analogous to D, but RXR antagonist HX531 (3 μM) was applied to triplication neurons. N = 4. **F** qPCR analysis of SCD1 and SCD5 mRNA levels in induced M17D/αS::YFP cells, vehicle (Dox)- vs. LG1069-treated (2 μM; Dox/LG1069). N = 3. **G** qPCR analysis of SCD5 mRNA levels in αS triplication iPSC neurons, vehicle (−)− vs. LG1069-treated (1 μM; LG1069). N = 3. **H** Analogous to D, but WB analysis of perilipin-2 (Plin2) and GAPDH; quantitation of Plin2/GAPDH ratio relative to untreated control (−). N = 3. All data are mean ± SD. *ns* not significant, *$p < 0.05$. **$p < 0.01$. ***$p < 0.001$. ****$p < 0.0001$

LG1069 also led to a decrease in LD-associated protein, perilipin-2 in the triplication neurons (Fig. 3H) [76].

Next, we assessed the implication of RXR agonism on altered FA desaturase activity of SCD and FADS2, when considered together. The slight increase in SCD activity in conjunction with substantial reduction of FADS2 activity (Fig. 3A) points toward an altered MUFA/PUFA balance upon RXR-activation. In the phospholipid membrane, incorporation of MUFAs can lead to displacement of PUFAs. This is associated with reduced lipid peroxidation, resulting in improved cellular health [77, 78]. To assess this aspect, we studied the widely used marker 4-Hydroxynonenal (4-HNE) as a proxy for lipid peroxidation. A reduction in 4-HNE signal was observed

upon LG1069 treatment in both αS-expressing human neural cells (Supplementary Fig. 2A) and patient αS triplication neurons (Supplementary Fig. 2B).

Activation of RXR reduces αS accumulation in human neural cells

Given the importance of αS in PD/DLB, we asked whether RXR activation impacts αS per se (Fig. 4A). M17D human

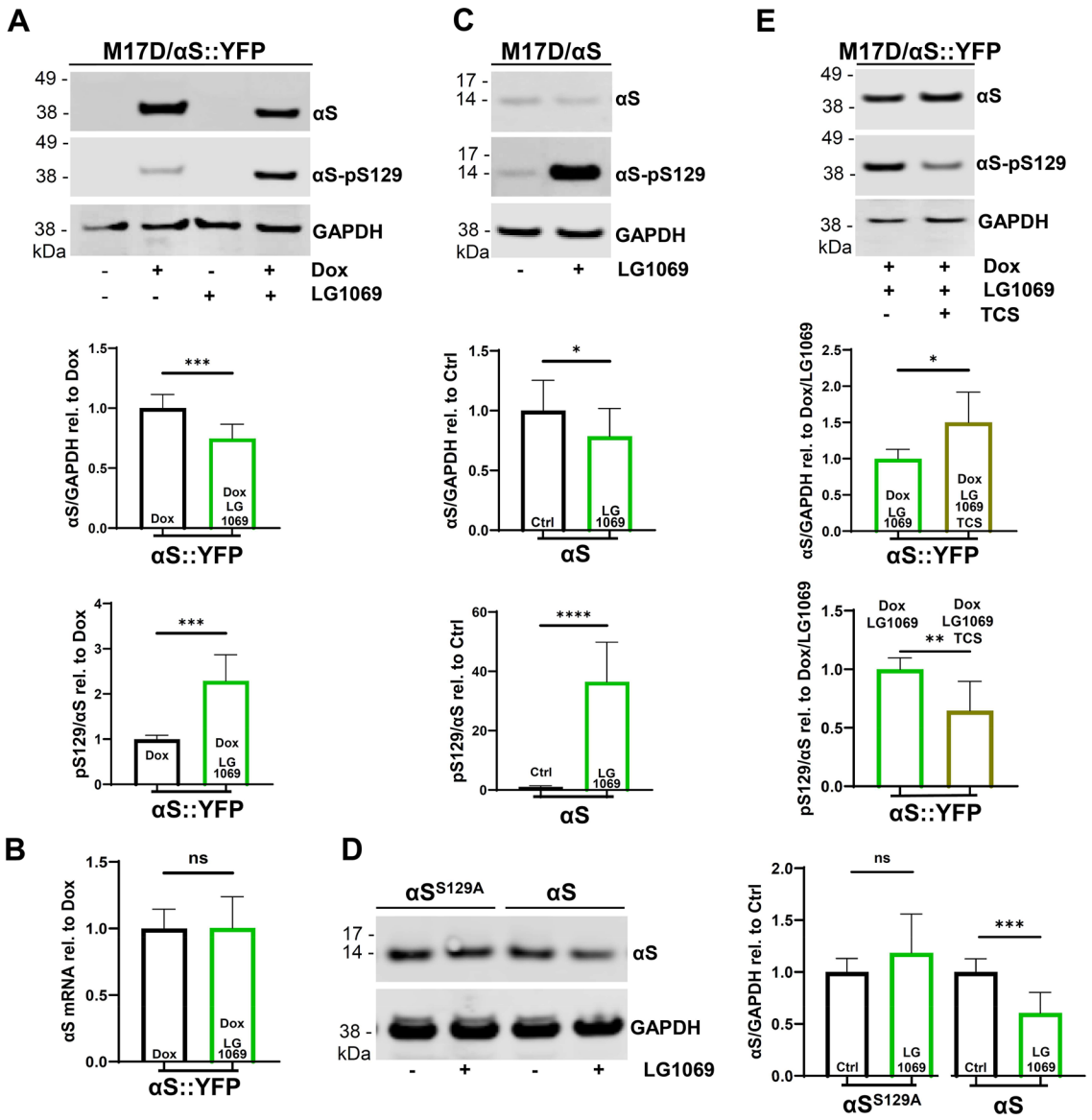

Fig. 4 LG1069 lowers αS protein level with concomitant rise in phosphorylation at S129. **A** Top, uninduced and induced M17D/αS::YFP cells were treated with vehicle or the RXR activator LG1069 (1 µM). WB to total αS (mAb 15G7), pS129 αS (pAb MJFR-13), and GAPDH as a loading control. Middle, αS/GAPDH ratios of Dox-induced vehicle-treated (Dox, set to 1) vs. LG1069-treated cells (Dox, LG1069). Bottom, pS129/total αS ratios for the same samples as in the middle panel. N = 4. **B** Quantitative PCR (qPCR) analysis of αS mRNA in Dox-induced M17D/αS::YFP cells treated with vehicle (Dox, set to 1) or 1 µM RXR activator LG1069 (Dox, LG1069). N = 3. **C** Constitutively expressing M17D/αS cells were treated with vehicle or the RXR activator LG1069 (4 µM). WB to total αS (mAb 15G7), pS129 αS (pAb MJFR-13), and GAPDH (loading control). Middle, αS/GAPDH ratios of vehicle-treated (set to 1) vs. LG1069-treated cells. N = 6. Bottom, pS129/total αS ratios analogous to the middle panel. N = 3. **D** Left, M17D human neural cells transfected with αS 129A (phospho-deficient) or WT treated with vehicle or the RXR activator LG1069 (2 µM). WB to total αS (mAb 15G7) and GAPDH. Right, αS/GAPDH ratios of all 4 conditions. N = 3. **E** Top, WB to total αS (mAb 15G7), pS129 αS (pAb MJFR-13), and GAPDH for Dox-induced M17D/αS::YFP cells treated with LG1069 in absence (Dox/LG1069) or presence of 0.1 µM Plk2 inhibitor TCS7005 (Dox/LG1069/TCS). Middle, quantitation of αS/GAPDH ratios. Bottom, pS129/total αS ratios. N = 3. All data are mean ± SD. *ns* not significant, $*p < 0.05$. $**p < 0.01$. $***p < 0.001$. $****p < 0.0001$

neural cells expressing αS::YFP were treated with vehicle or LG1069, and lysates were probed for total αS and phosphoserine-129 αS (pS129) by WB (Fig. 4A). Strikingly, LG1069 treatment reduced αS levels. This was concomitant with a rise in pS129 relative to untreated cells (Fig. 4A). To ascertain whether the loss in αS signal was a result of transcriptional repression or protein turnover, we subjected the vehicle- and LG1069-treated cells to qPCR. No significant change was observed in αS transcript levels (Fig. 4B), indicating that LG1069 treatment alters αS at the protein level. Cells treated with the HX630 agonist similarly showed reduced αS levels and increased pS129 vs. untreated cells (Supplementary Fig. 3). To validate that the effect of RXR agonism on αS is independent of dox induction and presence of the YFP tag, we next treated M17D cells that stably express untagged αS. Exposure to LG1069 again led to a decrease in αS levels and an increase in pS129 (Fig. 4C).

To investigate the participation of pS129 in the LG1069-mediated down-regulation of αS, we used two complementary approaches: (i) a mutational approach by converting serine-129 to alanine (S129A mutant); and (ii) a pharmacological approach by using a potent inhibitor, TCS7005, of Plk2 activity [79]. Plk2 is a serine/threonine kinase known to phosphorylate αS at position S129 [80, 81]. We first expressed either WT or S129A mutant αS in human neural M17D cells for 48 h prior to LG1069 treatment. 24 h post-treatment, WB revealed decreased αS WT levels relative to vehicle alone, as expected, while S129A abrogated the αS-lowering effect of LG1069 (Fig. 4D). Next, when the Plk2 inhibitor TCS7005 was added to LG1069-treated αS::YFP cells, we observed a reduction in pS129 levels and rise in αS level (Fig. 4E). Together, these data indicate that the LG1069-mediated lowering of αS levels is dependent on Plk2 activity and associated with S129 phosphorylation.

RXR agonist promotes lysosomal clearance of αS in human neural cells

The ubiquitin–proteasome system (UPS) and the autophagy-lysosomal pathway (ALP) are the major degradation pathways that cells use to maintain protein homeostasis. While the UPS degrades most short-lived proteins [82], the ALP is involved in the bulk degradation process by which longer-lived macromolecules and dysfunctional organelles can be cleared [83]. To determine whether the ALP is involved in the RXR-mediated reduction of αS, we used a targeted strategy. First, we asked whether acidic lysosome content in cells was influenced by LG1069 treatment. We labeled LG1069-treated and untreated αS::YFP-expressing M17D human neural cells with LysoTracker Red, a fluorescent dye that labels acidic cellular compartments, most notably, lysosomes. Quantification of the LysoTracker fluorescence intensity revealed a significant increase in LG1069-treated cells relative to untreated cells (Fig. 5A). We then examined two commonly used markers of the ALP pathway, p62 and microtubule-associated protein 1B light chain-3 II(LC3II). Quantitative WBs of LC3II and p62 in lysates of LG1069-treated vs. untreated cells showed an increase in LC3II and a decrease in p62 levels (Fig. 5B and C). To corroborate these findings, we tested whether pharmacological ALP inhibition would alter the observed reduction of αS by LG1069. For this purpose, we chose 3-methyladenine (3-MA) and ammonium chloride (AmCl), two widely used ALP inhibitors [84]. Treatment with AmCl in the presence of LG1069 led to an increase in αS levels and a decrease in pS129 signal when compared to LG1069-only treated cells (Fig. 5D). A closely similar effect was observed upon treatment with 3-MA in presence of LG1069 (Fig. 5E). Our results indicate that LG1069 enhances lysosomal clearance of αS in M17D human neural cells.

Pharmacological RXR activation triggers lysosomal αS clearance in patient-derived αS triplication neurons

We next analyzed PD patient iPSC-derived αS triplication neurons reflecting the chronic and endogenous αS state. We differentiated αS triplication and corrected control neurons to DIV17 and assayed total and pS129 αS levels in the absence or presence of LG1069 by WB (Fig. 6A). Upon treatment with LG1069, no significant change in αS levels or pS129 was observed in the control neurons (Fig. 6A). However, in triplication neurons, LG1069 induced a decrease in total αS levels and a relative rise in pS129 levels compared to vehicle control (Fig. 6A). Conversely, treating the αS triplication neurons with the RXR antagonist HX531, increased αS levels and decreased pS129 relative to vehicle control (Fig. 6B). LG1069 modestly reduced LDH release while the RXR antagonist HX531 increased its release (Supplementary Fig. 4A and 4B, respectively). Collectively, these data show that RXR signaling modulates levels of endogenous αS in PD patient neurons and alleviates cytotoxicity. Given the rise in pS129 upon LG1069-treatment, we investigated the participation of Plk2 kinase. Pharmacological interference using the small-molecule BI2536, which potently inhibits Plk2 activity [85], led to a significant decrease in pS129 signal and a reversal of the LG1069-mediated reduction of αS (Fig. 6C). These results are fully in line with our outcomes in M17D human neural cells (Fig. 4E). Given our observation in the M17D human neural cells that the lysosomal pathway is involved in αS turn-over, we asked if markers associated with this pathway such as p62, LC3 and LAMP1 are also altered in the triplication neurons upon LG1069-treatment. Comparison of LG1069- to vehicle-treated neurons showed a decrease in p62 (Fig. 6D), an elevation of LC3 (Fig. 6E),

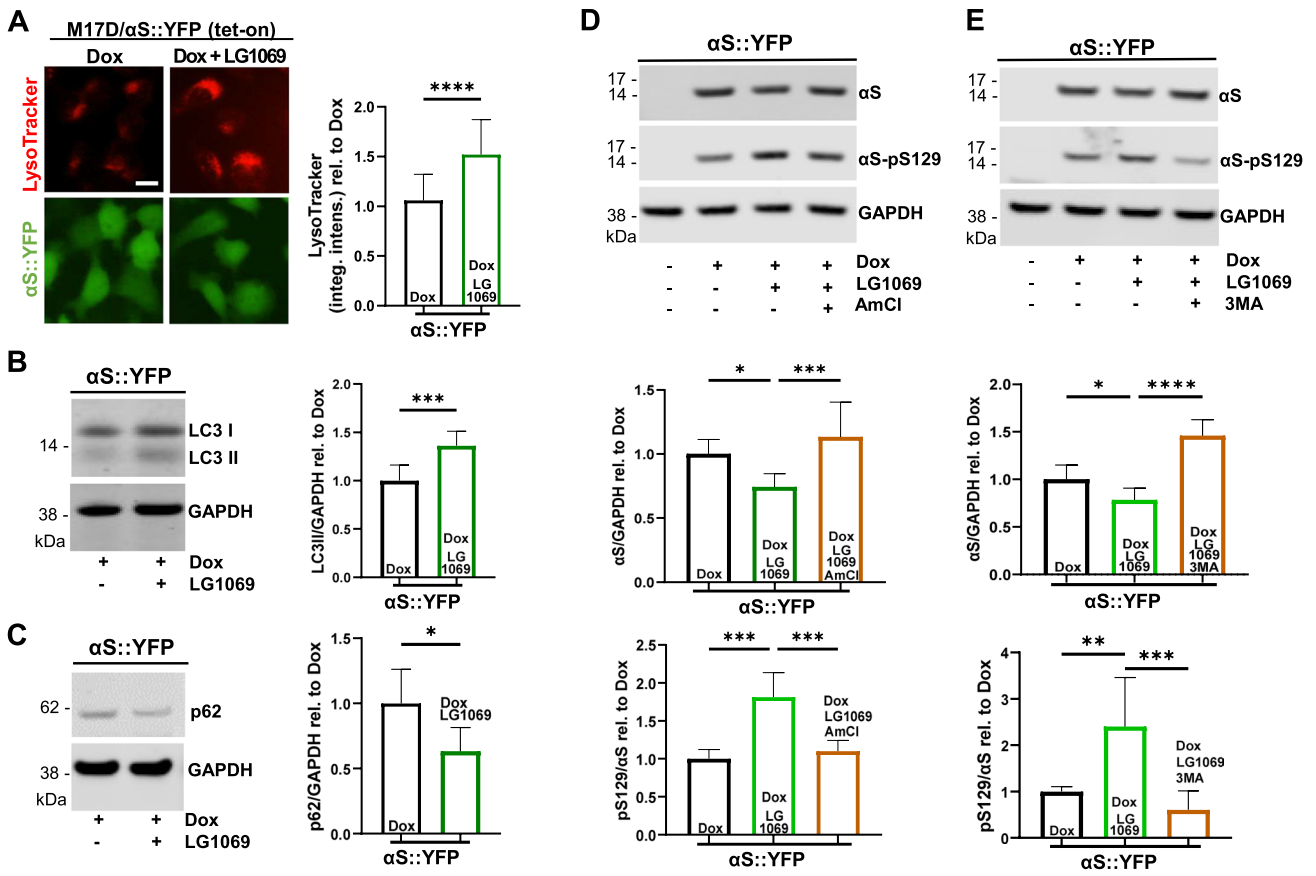

Fig. 5 RXR signaling pathway mediates lysosomal clearance of αS. **A** Left, induced M17D/αS::YFP human neural cells were treated with vehicle or the RXR activator LG1069 (1 μM) for 72 h. Visualization of lysosomal content (LysoTracker; red) and αS::YFP fluorescence images (green) at $t = 72$ h. Scale bar, 25 μm. Right, quantification of LysoTracker signal integrated intensity relative to vehicle treatment (set to 1). N = 4. **B** Left, Analogous to A, but WB to LC3 and GAPDH (loading control). Right, quantification of LC3II/GAPDH ratios relative to vehicle treatment (set to 1). N = 4. **C** Analogous to B, but WB to p62 and GAPDH. Quantification of p62/GAPDH ratios relative to vehicle treatment (set to 1). N = 2. **D** Top, induced M17D/αS::YFP cells were treated with vehicle, LG1069 (2 μM) or LG1069 (2 μM) + ammonium chloride (AmCl, 30 mM). WB to total αS (mAb 15G7), pS129 αS (pAb MJFR-13), and GAPDH (loading control). Middle, quantification of αS/GAPDH ratios relative to vehicle treatment (set to 1). Bottom, pS129/total αS ratios relative to vehicle treatment (set to 1). N = 3. **E** Analogous to D, but 3MA (10 mM) instead of AmCl was used. Top, WB. Middle, quantification of αS/GAPDH ratios relative to vehicle treatment (set to 1). Bottom, pS129/total αS ratios relative to vehicle treatment (set to 1). N = 4. All data are mean ± SD. $^{*}p < 0.05$. $^{**}p < 0.01$. $^{***}p < 0.001$. $^{****}p < 0.0001$

and increased levels of endogenous LAMP1 visualized by immunofluorescence microscopy (Fig. 6F). Taken together these observations suggest that RXR activation promotes lysosomal clearance of endogenous αS in PD patient triplication neurons.

Discussion

The preponderance of genetic, GWAS, and histopathological evidence highlights both the synaptic protein αS and aberrations in lipid metabolism as key players in PD pathobiology. Therefore, modulating both αS biology and lipid metabolism could serve as useful strategies for therapeutic intervention in PD and other synucleinopathies. Here, we focus on modulating the RXR nuclear receptor signaling pathway and assess its impact on both αS and FA/lipid biology in cellular models of PD.

NRs form a unique superfamily of transcription factors that bind intracellular ligands and cell-permeable extracellular ligands directly. Thus, activated NRs have the capability to translate both environmental changes and intracellular metabolic alterations into distinct physiological responses by regulating gene expression. Malfunctioning NRs cause a wide array of diseases and inherited disorders [43, 86]. Their ligand-responsive nature renders NRs susceptible to modulation by synthetic ligands, which currently make up nearly 16% of all FDA-approved drugs [87].

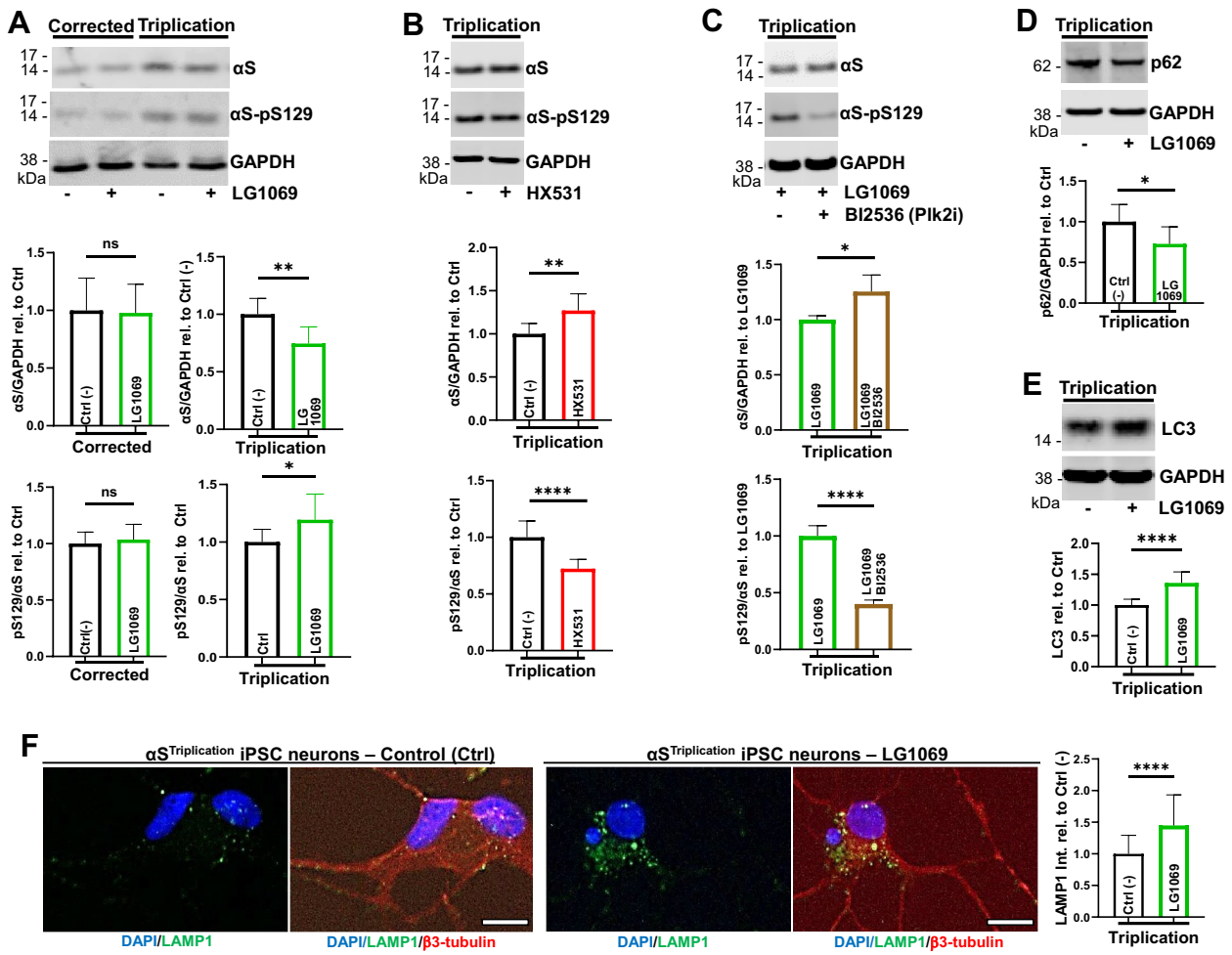

Fig. 6 Treatment of PD patient-derived αS triplication neurons with RXR pathway modulators. **A** Top, WB to total αS (mAb 4B12), phospho-serine129 αS (pAb D1R1R) and GAPDH (loading control) levels in patient-derived αS triplication iPSC neurons and isogenic control (Corrected), vehicle vs. LG1069-treated (1 µM). Middle, quantification of total αS/GAPDH ratios, relative to the respective vehicle control (set to 1). Bottom, pS129/total αS ratios relative to vehicle treatment (Ctrl, set to 1). N = 4. **B** Analogous to A, but 3 µM RXR antagonist HX531 was applied to triplication patient neurons. Middle, αS/GAPDH ratios relative to vehicle treatment (Ctrl, set to 1). Bottom, pS129/total αS levels relative to vehicle treatment (Ctrl, set to 1). N = 4. **C** αS triplication neurons treated with LG1069 (1 µM) or LG1069 (1 µM) plus Plk2 inhibitor BI2536 (Plk2i, 0.5 µM). WB to total αS (mAb 4B12), pS129 αS (pAb D1R1R), and GAPDH (loading control). Middle, quantification of αS/GAPDH ratios relative to LG1069 treatment (set to 1). Bottom, pS129/total αS ratios relative to LG1069 treatment (set to 1). N = 2. **D** Analogous to A, but WB to p62 and GAPDH. Quantification of p62/GAPDH ratios relative to vehicle treatment (Ctrl, set to 1) in αS triplication neurons. N = 2. **E** Analogous to D, but WB to LC3 and GAPDH. Quantification of LC3/GAPDH ratios relative to vehicle treatment (Ctrl). N = 3. **F** αS triplication neurons, vehicle (Ctrl, left two images) vs. LG1069 (right two images). LAMP1 immunofluorescence (IF; green) or LAMP1 + β3-tubulin IF (red); nuclei were visualized via DAPI staining (blue). Scale bar, 15 µm. Quantification of LAMP1 integrated intensity relative to vehicle (Ctrl). N = 3. All data are mean ± SD. *ns* not significant, *$p < 0.05$. **$p < 0.01$. ****$p < 0.0001$

To evaluate RXR signaling in PD-relevant cellular models, we leveraged the availability of several different small-molecule activators (LG1069/bexarotene, LG754, and HX630) and an RXR-antagonist, HX531, in our well-validated Dox-inducible αS::YFP expression system [56] in M17D human neural cells and PD patient-derived neurons. We found that RXR agonism using the aforementioned activators ameliorates αS-induced cytotoxicity as evidenced by a reduction in LDH release (Fig. 1B–D). In contrast, treatment with the HX531 antagonist worsened αS-associated cytotoxicity (Fig. 1E). The elevated toxicity seen upon αS expression was accompanied by LD abundance (Fig. 2A). This is in keeping with studies in multiple model systems ranging from yeast and *Drosophila* to rodent neurons, where expression of αS leads to LD accumulation [37–39]. In primary cortical neurons, a connection between αS cytotoxicity, lipids, and LD has also been reported [37]. In addition, a number of PD patient brains have been reported to

have significant neuronal LD accumulation by postmortem examination [41]. Interestingly, treatment of αS-expressing M17D human neural cells with RXR agonists (LG1069 and HX630; Fig. 2A–B) reversed the αS-triggered increase in LD size, while pharmacological inhibition of RXR activity with the antagonist HX531 led to a further increase in LD size (Fig. 2C). These results suggest that both αS and RXR pathway can influence LDs. We previously identified TG and diglyceride abundance to be associated with excess cellular αS and the accumulation of LDs [37]. Therefore, we asked if the reduction in LD size might influence cellular TGs and found a significant decrease in total cellular TGs upon treatment with LG1069 (Fig. 2D), suggesting that LD size serves as an indicator of TGs in the context of RXR activation [88].

NR agonists have been reported to modulate FA desaturases such as SCD and FADS2 [70–72]. FA desaturases play an important role in mobilizing cellular lipids. Our unbiased lipidomic approach revealed that activated RXR strikingly decreased FADS2 activity, and mildly increased the desaturation index of MUFAs, i.e., SCD activity (Fig. 3A). A decrease in FADS2 activity has been linked to reduced FA re-esterification [73]; in the RXR agonism paradigm, this could potentially limit re-formation of TGs. One adverse outcome of RXR agonism could be build-up of free FAs leading to lipotoxicity. However, we did not see evidence of overt cytotoxicity of RXR activation in our cellular models of PD. Instead, we observed reduced cytotoxicity upon RXR-activation (Fig. 1B–D, Supplementary Fig. 4A–B). We favor a scenario where FAs can potentially be channeled upon RXR agonism to improve FA oxidation. In support, LG1069-activated NR have been documented to improve mitochondrial oxidative metabolism and bioenergetics, leading to neuroprotection in a mouse model of Huntington's disease [51]. However, additional studies are required to assess whether RXR modulation causes this effect in αS PD models.

In addition to FADS2, we found that RXR agonism differentially impacts the two human isoforms of SCD, SCD1 and SCD5. While SCD1 levels were elevated, those of SCD5 were downregulated by RXR agonist (Fig. 3). Upregulation of SCD1 has also been noted upon ablation of SCD2 (murine ortholog of human SCD5) in mice [87]. Increased SCD1 levels likely explain the observed rise in the MUFA (C16, C18) desaturation index upon RXR activation (Fig. 3A). This is not entirely unexpected, since a similar rise in SCD1 transcript was seen upon LG1069 administration in a model of Huntington's disease [51]. A decrease in SCD5 level by RXR agonism makes this homolog an unlikely contributor to the increased MUFA desaturation index. However, we see a concurrent decrease in LD size upon RXR agonism (Fig. 2A–B), potentially supporting a role of SCD5 in LD function. This observation is in keeping with a study that identified SCD5 in a screen of ~ 18,000 human genes as a gene whose reduction leads to smaller LDs [89]. In corroboration, we also find that levels of perilipin-2, an LD-associated protein, is reduced in LG1069-treated patient neurons (Fig. 3H). Our study is the first report connecting SCD5 to LD in presence of RXR activation. The differential effects on FA desaturases SCD and FADS2 imposed by RXR agonism indicated an altered MUFA and PUFA balance in the cell. Our data raise the possibility that modest MUFA accumulation by virtue of increased SCD activity in conjunction with reduced FADS2 (PUFA) activity could decrease lipid oxidation, thereby reversing one toxic mechanism by which αS may cause cellular stress. In support, we found that activation of RXR leads to reduced 4-HNE signal (Supplementary Fig. 2A–B). This would predict an associated reduction in cytotoxicity. In agreement, we found an improvement in membrane integrity and cell viability upon treatment with several RXR-agonists (Fig. 1; Supplementary Fig. 4A). Our data reveal a previously uncharacterized connection between FA desaturases (SCD, FADS2) and lipid oxidation as effects of RXR agonism [90].

αS is strongly implicated in the pathogenesis of PD. Strikingly, we found that RXR agonists reduced the protein levels of αS in both our models: M17D human neural cells and PD patient-derived triplication neurons (Fig. 4A; 6A; Supplementary Fig. 3). This effect was reversed with use of the RXR antagonist HX531 (Fig. 6B). Collectively, these data provide the first evidence of RXR signaling influencing αS turnover in cellular models of PD. Concurrent with decreased αS levels upon RXR-activation, our data revealed a rise in phosphorylation of αS at residue S129 (Figs. 4A, C; 6A). This pattern was reversed by the antagonist HX531 (Fig. 6B). Pharmacological inhibition of Plk2 negated the effect of RXR pathway activation on αS and pS129 (Figs. 4E; 6C). In accord, the phosphorylation-preventing S129A αS mutant lost its ability to be downregulated by RXR agonism (Fig. 4D). These data implicate pS129 and associated Plk2 kinase activity in mediating αS turnover. While pS129 has been largely associated with neurotoxicity and pathology by virtue of its occurrence in LBs/LNs, emerging evidence suggests a physiological role separate from that in LB pathology. For example, brain pS129 is elevated in environmentally enriched mice exhibiting enhanced hippocampal long-term potentiation [91]. Neuronal stimulation also enhances Plk2 kinase activity that triggers a sustained increase of pS129 in cultured neurons without overt cytotoxicity [91]. In the latter study, pS129 appeared to fine-tune the balance between excitatory and inhibitory neuronal currents. In yeast, the non-phosphorylatable form of αS, S129A, is more toxic and forms more inclusions than does its WT counterpart [92], suggesting that serine 129 phosphorylation is beneficial in this scenario. In addition, in a rodent PD model [93], S129A expression exacerbates

αS-induced nigral pathology, whereas phosphorylated αS attenuates αS-induced nigrostriatal degeneration. As for RXR-mediated pS129 accumulation, further work is needed to understand how Plk2 becomes activated to modulate αS phosphorylation.

To delineate the pathway for αS turnover, we altered the lysosomal degradation pathway with either 3-MA or ammonium chloride as pharmacological inhibitors. Both compounds abrogated the RXR agonism effects (Fig. 5D–E). We found several indications of lysosomal pathway activation upon RXR activation such as an increase in LysoTracker staining, increased autophagy-lysosomal marker LC3, elevated LAMP1 intensity, and decreased p62 levels (Figs. 5A–C; 6D–F). Taken together, our data suggest that RXR activation triggers lysosomal clearance of αS and is associated with a rise in pS129. In line with our observations, blocking S129 phosphorylation has been reported to cause impaired autophagic clearance of αS in yeast [94]. Moreover, in mammalian cells and rodents, increasing the level of pS129 by overexpressing Plk2 promoted lysosomal degradation of αS [85]. Suppression of dopaminergic neurodegeneration and reversal of motor impairments were also observed in this Plk2 over-expressing rodent model, supporting a beneficial role of pS129.

As an FDA-approved drug for T-cell lymphoma, the RXR agonist LG1069/bexarotene, has been explored in models of Alzheimer's disease, Huntington disease, ALS, and a 6-OHDA toxin-based PD model, with various reports of improvements in behavioral symptoms, memory, neuronal loss, and neurotrophic signaling (48, 51–53, 95, 96). However, RXR pathway activation has been under explored in αS-based models relevant to PD/DLB. Our study in cellular models of PD-relevant αS dyshomeostasis is a novel step in this direction. Here, we have not only used the widely reported agonist LG1069/bexarotene as proof of principle but also utilized other agonists and an antagonist to quantify the consequences of the RXR signaling pathway relevant to lipid metabolism and αS homeostasis. RXR partners with other NR to manifest its effects, so we will next determine the heterodimeric partner for RXR in mediating the observed effects and help target more molecularly specific pathways. We will also focus on dissecting the influence of RXR activation on other genetic and sporadic forms of synucleinopathy. Finally, we will search for in vivo efficacy of appropriate small-molecule RXR agonists in PD mouse models to establish potential clinical suitability.

Supplementary Information The online version contains supplementary material available at https://doi.org/10.1007/s00018-024-05373-2.

Acknowledgements We thank members of the Dettmer Lab (BWH/HMS), Selkoe Lab (BWH/HMS), Vikram Khurana (BWH/HMS), Silke Nuber (BWH/HMS) and their lab members and Saranna Fanning (BWH/HMS) for advice and/or discussions; Jouri Elsadek for technical support; Lai Ding and the NeuroTechnology Studio at BWH for providing access to the Incucyte, InCell machines and consultation on data analysis; Stephanie Soriano-Cruz and Christina R Muratore at Neurohub/BWH for providing patient-derived cell lines and consultation, and R. Brathwaite and G. Dove for administrative assistance. We thank Kevin Hodgetts for consultation and advice. We acknowledge the input of Scott Splett at OmegaQuant for FA analysis. We thank members of the Karolinska-Harvard Collaborative Program on Parkinson's Disease for discussion.

Author contributions A.T. designed the study with advice from U.D. and D.J.S. A.T., H.A., and L.B. performed experiments and data analysis. A.T., H.A., U.D., and D.J.S. analyzed, interpreted data and further designed follow-up experiments. A.T. wrote the first draft. A.T., U.D., and D.J.S revised and wrote the final manuscript. All authors read and approved the final manuscript.

Funding This work was supported by the National Institutes of Health (NS099328 to U.D, NS083845 to D.J.S.) and a philanthropic gift establishing the Karolinska-Harvard Collaboration on Parkinson's Disease. The funders had no role in study design, data collection and analysis, decision to publish, or preparation of the manuscript.

Availability of data and materials All analyzed data during this study are included in this published article (and its supplementary information files).

Declarations

Conflict of interest D.S. is a director and consultant to Prothena Biosciences. The remaining authors declare no competing financial interests.

Ethics approval and consent to participate Not applicable.

Consent for publication Not applicable.

References

1. Spillantini MG, Schmidt ML, Lee VM, Trojanowski JQ, Jakes R, Goedert M (1997) Alpha-synuclein in Lewy bodies. Nature 388(6645):839–840
2. Parkinson's Foundation. https://www.parkinson.org/understanding-parkinsons/statistics Accessed 23 September 2023.

3. Parkinson J (2002) An essay on the shaking palsy. 1817. J Neuropsychiatry Clin Neurosci 14(2):223–36; discussion 222.
4. Nalls MA, Blauwendraat C, Vallerga CL, Heilbron K, Bandres-Ciga S, Chang D et al (2019) Identification of novel risk loci, causal insights, and heritable risk for Parkinson's disease: a meta-analysis of genome-wide association studies. Lancet Neurol 18(12):1091–1102
5. Brockmann K, Schulte C, Hauser AK, Lichtner P, Huber H, Maetzler W et al (2013) SNCA: major genetic modifier of age at onset of Parkinson's disease. Mov Disord Off J Mov Disord Soc 28(9):1217–1221
6. Edwards TL, Scott WK, Almonte C, Burt A, Powell EH, Beecham GW et al (2010) Genome-wide association study confirms SNPs in SNCA and the MAPT region as common risk factors for Parkinson disease. Ann Hum Genet 74(2):97–109
7. Polymeropoulos MH, Lavedan C, Leroy E, Ide SE, Dehejia A, Dutra A et al (1997) Mutation in the alpha-synuclein gene identified in families with Parkinson's disease. Science 276(5321):2045–2047
8. Krüger R, Kuhn W, Müller T, Woitalla D, Graeber M, Kösel S et al (1998) Ala30Pro mutation in the gene encoding alpha-synuclein in Parkinson's disease. Nat Genet 18(2):106–108
9. Zarranz JJ, Alegre J, Gómez-Esteban JC, Lezcano E, Ros R, Ampuero I et al (2004) The new mutation, E46K, of alpha-synuclein causes Parkinson and Lewy body dementia. Ann Neurol 55(2):164–173
10. Appel-Cresswell S, Vilarino-Guell C, Encarnacion M, Sherman H, Yu I, Shah B, et al (2013) Alpha-synuclein p.H50Q, a novel pathogenic mutation for Parkinson's disease. Mov Disord Off J Mov Disord Soc 28(6):811–813
11. Lesage S, Anheim M, Letournel F, Bousset L, Honoré A, Rozas N et al (2013) G51D α-synuclein mutation causes a novel parkinsonian-pyramidal syndrome. Ann Neurol 73(4):459–471
12. Kiely AP, Ling H, Asi YT, Kara E, Proukakis C, Schapira AH et al (2015) Distinct clinical and neuropathological features of G51D SNCA mutation cases compared with SNCA duplication and H50Q mutation. Mol Neurodegener 10:41
13. Pasanen P, Myllykangas L, Siitonen M, Raunio A, Kaakkola S, Lyytinen J et al (2014) Novel α-synuclein mutation A53E associated with atypical multiple system atrophy and Parkinson's disease-type pathology. Neurobiol Aging 35(9):2180.e1–5
14. Yoshino H, Hirano M, Stoessl AJ, Imamichi Y, Ikeda A, Li Y, et al (2017) Homozygous alpha-synuclein p.A53V in familial Parkinson's disease. Neurobiol Aging 57:248.e7–248.e12.
15. Liu H, Koros C, Strohäker T, Schulte C, Bozi M, Varvaresos S et al (2021) A novel SNCA A30G mutation causes familial Parkinson's disease. Mov Disord Off J Mov Disord Soc 36(7):1624–1633
16. Singleton AB, Farrer M, Johnson J, Singleton A, Hague S, Kachergus J et al (2003) Alpha-Synuclein locus triplication causes Parkinson's disease. Science 302(5646):841
17. Byers B, Cord B, Nguyen HN, Schüle B, Fenno L, Lee PC et al (2011) SNCA triplication Parkinson's patient's iPSC-derived DA neurons accumulate α-synuclein and are susceptible to oxidative stress. PLoS One 6(11):e26159
18. Devine MJ, Ryten M, Vodicka P, Thomson AJ, Burdon T, Houlden H et al (2011) Parkinson's disease induced pluripotent stem cells with triplication of the α-synuclein locus. Nat Commun 2:440
19. Chartier-Harlin MC, Kachergus J, Roumier C, Mouroux V, Douay X, Lincoln S et al (2004) Alpha-synuclein locus duplication as a cause of familial Parkinson's disease. Lancet Lond Engl 364(9440):1167–1169
20. Konno T, Ross OA, Puschmann A, Dickson DW, Wszolek ZK (2016) Autosomal dominant Parkinson's disease caused by SNCA duplications. Parkinsonism Relat Disord 22(Suppl 1):S1–S6
21. Laperle AH, Sances S, Yucer N, Dardov VJ, Garcia VJ, Ho R et al (2020) iPSC modeling of young-onset Parkinson's disease reveals a molecular signature of disease and novel therapeutic candidates. Nat Med 26(2):289–299
22. Wong YC, Krainc D (2017) α-synuclein toxicity in neurodegeneration: mechanism and therapeutic strategies. Nat Med 23(2):1–13
23. Stefanis L (2012) α-Synuclein in Parkinson's disease. Cold Spring Harb Perspect Med 2(2):a009399
24. Tripathi A, Fanning S, Dettmer U (2021) Lipotoxicity downstream of α-synuclein imbalance: a relevant pathomechanism in synucleinopathies? Biomolecules 12(1):40
25. Flores-Leon M, Outeiro TF (2023) More than meets the eye in Parkinson's disease and other synucleinopathies: from proteinopathy to lipidopathy. Acta Neuropathol (Berl) 146(3):369–385
26. Fanning S, Selkoe D, Dettmer U (2020) Parkinson's disease: proteinopathy or lipidopathy? NPJ Park Dis 6:3
27. Shahmoradian SH, Lewis AJ, Genoud C, Hench J, Moors TE, Navarro PP et al (2019) Lewy pathology in Parkinson's disease consists of crowded organelles and lipid membranes. Nat Neurosci 22(7):1099–1109
28. Gai WP, Yuan HX, Li XQ, Power JT, Blumbergs PC, Jensen PH (2000) In situ and in vitro study of colocalization and segregation of alpha-synuclein, ubiquitin, and lipids in Lewy bodies. Exp Neurol 166(2):324–333
29. Araki K, Yagi N, Ikemoto Y, Yagi H, Choong CJ, Hayakawa H et al (2015) Synchrotron FTIR micro-spectroscopy for structural analysis of Lewy bodies in the brain of Parkinson's disease patients. Sci Rep 5:17625
30. Moors TE, Maat CA, Niedieker D, Mona D, Petersen D, Timmermans-Huisman E et al (2021) The subcellular arrangement of alpha-synuclein proteoforms in the Parkinson's disease brain as revealed by multicolor STED microscopy. Acta Neuropathol (Berl) 142(3):423–448
31. Bodner CR, Dobson CM, Bax A (2009) Multiple tight phospholipid-binding modes of alpha-synuclein revealed by solution NMR spectroscopy. J Mol Biol. 390(4):775–90
32. Bodner CR, Maltsev AS, Dobson CM, Bax A (2010) Differential phospholipid binding of alpha-synuclein variants implicated in Parkinson's disease revealed by solution NMR spectroscopy. Biochemistry 49(5):862–871
33. Ruipérez V, Darios F, Davletov B (2010) Alpha-synuclein, lipids and Parkinson's disease. Prog Lipid Res 49(4):420–428
34. Stöckl M, Fischer P, Wanker E, Herrmann A (2008) Alpha-synuclein selectively binds to anionic phospholipids embedded in liquid-disordered domains. J Mol Biol 375(5):1394–1404
35. Sharon R, Goldberg MS, Bar-Josef I, Betensky RA, Shen J, Selkoe DJ (2001) alpha-Synuclein occurs in lipid-rich high molecular weight complexes, binds fatty acids, and shows homology to the fatty acid-binding proteins. Proc Natl Acad Sci USA 98(16):9110–9115
36. Karube H, Sakamoto M, Arawaka S, Hara S, Sato H, Ren CH et al (2008) N-terminal region of alpha-synuclein is essential for the fatty acid-induced oligomerization of the molecules. FEBS Lett 582(25–26):3693–3700
37. Fanning S, Haque A, Imberdis T, Baru V, Barrasa MI, Nuber S et al (2019) Lipidomic analysis of α-synuclein neurotoxicity identifies stearoyl CoA desaturase as a target for Parkinson treatment. Mol Cell 73(5):1001-1014.e8
38. Outeiro TF, Lindquist S (2003) Yeast cells provide insight into alpha-synuclein biology and pathobiology. Science 302(5651):1772–1775
39. Girard V, Jollivet F, Knittelfelder O, Celle M, Arsac JN, Chatelain G et al (2021) Abnormal accumulation of lipid droplets in neurons induces the conversion of alpha-Synuclein to proteolytic resistant forms in a Drosophila model of Parkinson's disease. PLoS Genet 17(11):e1009921
40. Smith LJ, Bolsinger MM, Chau KY, Gegg ME, Schapira AHV (2023) The GBA variant E326K is associated with alpha-synuclein

aggregation and lipid droplet accumulation in human cell lines. Hum Mol Genet 32(5):773–789
41. Brekk OR, Honey JR, Lee S, Hallett PJ, Isacson O (2020) Cell type-specific lipid storage changes in Parkinson's disease patient brains are recapitulated by experimental glycolipid disturbance. Proc Natl Acad Sci U S A 117(44):27646–27654
42. Evans RM, Mangelsdorf DJ (2014) Nuclear receptors, RXR, and the big bang. Cell 157(1):255–266
43. Moutinho M, Codocedo JF, Puntambekar SS, Landreth GE (2019) Nuclear receptors as therapeutic targets for neurodegenerative diseases: lost in translation. Annu Rev Pharmacol Toxicol 59:237–261
44. Sharma S, Shen T, Chitranshi N, Gupta V, Basavarajappa D, Sarkar S et al (2022) Retinoid X receptor: cellular and biochemical roles of nuclear receptor with a focus on neuropathological involvement. Mol Neurobiol 59(4):2027–2050
45. Willems S, Zaienne D, Merk D (2021) Targeting nuclear receptors in neurodegeneration and neuroinflammation. J Med Chem 64(14):9592–9638
46. Shulman AI, Mangelsdorf DJ (2005) Retinoid x receptor heterodimers in the metabolic syndrome. N Engl J Med 353(6):604–615
47. Pérez E, Bourguet W, Gronemeyer H, de Lera AR (2012) Modulation of RXR function through ligand design. Biochim Biophys Acta 1821(1):57–69
48. Cramer PE, Cirrito JR, Wesson DW, Lee CYD, Karlo JC, Zinn AE et al (2012) ApoE-directed therapeutics rapidly clear β-amyloid and reverse deficits in AD mouse models. Science 335(6075):1503–1506
49. Wang W, Nakashima KI, Hirai T, Inoue M (2019) Neuroprotective effect of naturally occurring RXR agonists isolated from Sophora tonkinensis Gagnep on amyloid-β-induced cytotoxicity in PC12 cells. J Nat Med. 73(1):154–62
50. Yuan C, Guo X, Zhou Q, Du F, Jiang W, Zhou X et al (2019) OAB-14, a bexarotene derivative, improves Alzheimer's disease-related pathologies and cognitive impairments by increasing β-amyloid clearance in APP/PS1 mice. Biochim Biophys Acta Mol Basis Dis 1865(1):161–180
51. Dickey AS, Sanchez DN, Arreola M, Sampat KR, Fan W, Arbez N, et al (2017) PPARδ activation by bexarotene promotes neuroprotection by restoring bioenergetic and quality control homeostasis. Sci Transl Med 9(419):eaal2332
52. Riancho J, Ruiz-Soto M, Berciano MT, Berciano J, Lafarga M (2015) Neuroprotective effect of bexarotene in the SOD1(G93A) mouse model of amyotrophic lateral sclerosis. Front Cell Neurosci 9:250
53. McFarland K, Spalding TA, Hubbard D, Ma JN, Olsson R, Burstein ES (2013) Low dose bexarotene treatment rescues dopamine neurons and restores behavioral function in models of Parkinson's disease. ACS Chem Neurosci 4(11):1430–1438
54. Friling S, Bergsland M, Kjellander S (2009) Activation of retinoid X receptor increases dopamine cell survival in models for Parkinson's disease. BMC Neurosci 10:146
55. Spathis AD, Asvos X, Ziavra D, Karampelas T, Topouzis S, Cournia Z et al (2017) Nurr1:RXRα heterodimer activation as monotherapy for Parkinson's disease. Proc Natl Acad Sci U S A 114(15):3999–4004
56. Tripathi A, Alnakhala H, Terry-Kantor E, Newman A, Liu L, Imberdis T et al (2022) Pathogenic mechanisms of cytosolic and membrane-enriched α-synuclein converge on fatty acid homeostasis. J Neurosci Off J Soc Neurosci 42(10):2116–2130
57. Dettmer U, Newman AJ, von Saucken VE, Bartels T, Selkoe D (2015) KTKEGV repeat motifs are key mediators of normal α-synuclein tetramerization: Their mutation causes excess monomers and neurotoxicity. Proc Natl Acad Sci USA 112(31):9596–9601
58. Chen Y, Dolt KS, Kriek M, Baker T, Downey P, Drummond NJ et al (2019) Engineering synucleinopathy-resistant human dopaminergic neurons by CRISPR-mediated deletion of the SNCA gene. Eur J Neurosci 49(4):510–524
59. Zhang Y, Pak C, Han Y, Ahlenius H, Zhang Z, Chanda S et al (2013) Rapid single-step induction of functional neurons from human pluripotent stem cells. Neuron 78(5):785–798
60. Pang ZP, Yang N, Vierbuchen T, Ostermeier A, Fuentes DR, Yang TQ et al (2011) Induction of human neuronal cells by defined transcription factors. Nature 476(7359):220–223
61. TARGRETIN (bexarotene) capsules, for oral use Initial U.S. Approval: 1999'. 2015. Food and Drug Administration, Accessed 26 September 2023. https://www.accessdata.fda.gov/drugsatfda_docs/label/2015/021055s010lbl.pdf.
62. Zhang H, Jarjour AA, Boyd A, Williams A (2011) Central nervous system remyelination in culture–a tool for multiple sclerosis research. Exp Neurol 230(1):138–148
63. Cesario RM, Klausing K, Razzaghi H, Crombie D, Rungta D, Heyman RA et al (2001) The rexinoid LG100754 is a novel RXR:PPARgamma agonist and decreases glucose levels in vivo. Mol Endocrinol Baltim Md 15(8):1360–1369
64. Kanayasu-Toyoda T, Fujino T, Oshizawa T, Suzuki T, Nishimaki-Mogami T, Sato Y et al (2005) HX531, a retinoid X receptor antagonist, inhibited the 9-cis retinoic acid-induced binding with steroid receptor coactivator-1 as detected by surface plasmon resonance. J Steroid Biochem Mol Biol 94(4):303–309
65. Varga T, Czimmerer Z, Nagy L (2011) PPARs are a unique set of fatty acid regulated transcription factors controlling both lipid metabolism and inflammation. Biochim Biophys Acta 1812(8):1007–1022
66. Klemann CJHM, Martens GJM, Sharma M, Martens MB, Isacson O, Gasser T et al (2017) Integrated molecular landscape of Parkinson's disease. NPJ Park Dis 3:14
67. Alecu I, Bennett SAL (2019) Dysregulated lipid metabolism and its role in α-synucleinopathy in Parkinson's disease. Front Neurosci 13:328
68. Olzmann JA, Carvalho P (2019) Dynamics and functions of lipid droplets. Nat Rev Mol Cell Biol 20(3):137–155
69. Bresgen N, Kovacs M, Lahnsteiner A, Felder TK, Rinnerthaler M (2023) The janus-faced role of lipid droplets in aging: insights from the cellular perspective. Biomolecules 13(6):912
70. Miller CW, Ntambi JM (1996) Peroxisome proliferators induce mouse liver stearoyl-CoA desaturase 1 gene expression. Proc Natl Acad Sci U S A 93(18):9443–9448
71. Samuel W, Kutty RK, Nagineni S, Gordon JS, Prouty SM, Chandraratna RA et al (2001) Regulation of stearoyl coenzyme A desaturase expression in human retinal pigment epithelial cells by retinoic acid. J Biol Chem 276(31):28744–28750
72. Darabi M, Byagowi S, Fayezi S, Darabi M, Mirshahvaladi S, Sahmani M (2013) Transcriptional regulation of Δ6-desaturase by peroxisome proliferative-activated receptor δ agonist in human pancreatic cancer cells: role of MEK/ERK1/2 pathway. ScientificWorldJournal 2013:607524
73. Wang C, MacIntyre B, Mutch DM (2022) Inhibition of Δ-6 desaturase reduces fatty acid re-esterification in 3T3-L1 adipocytes independent of changes in n3-PUFA cellular content. Biochim Biophys Acta Mol Cell Biol Lipids 1867(7):159160
74. Shi X, Li J, Zou X, Greggain J, Rødkær SV, Færgeman NJ et al (2013) Regulation of lipid droplet size and phospholipid composition by stearoyl-CoA desaturase. J Lipid Res 54(9):2504–2514
75. Zhang L, Ge L, Parimoo S, Stenn K, Prouty SM (1999) Human stearoyl-CoA desaturase: alternative transcripts generated from a single gene by usage of tandem polyadenylation sites. Biochem J. 340(Pt 1):255–64
76. Wang J, Yu L, Schmidt RE, Su C, Huang X, Gould K et al (2005) Characterization of HSCD5, a novel human stearoyl-CoA

desaturase unique to primates. Biochem Biophys Res Commun 332(3):735–742
77. Rodencal J, Dixon SJ (2023) A tale of two lipids: Lipid unsaturation commands ferroptosis sensitivity. Proteomics 23(6):e2100308
78. Kim JW, Lee JY, Oh M, Lee EW (2023) An integrated view of lipid metabolism in ferroptosis revisited via lipidomic analysis. Exp Mol Med 55(8):1620–1631
79. Hanan EJ, Fucini RV, Romanowski MJ, Elling RA, Lew W, Purkey HE et al (2008) Design and synthesis of 2-amino-isoxazolopyridines as Polo-like kinase inhibitors. Bioorg Med Chem Lett 18(19):5186–5189
80. Inglis KJ, Chereau D, Brigham EF, Chiou SS, Schöbel S, Frigon NL et al (2009) Polo-like kinase 2 (PLK2) phosphorylates alpha-synuclein at serine 129 in central nervous system. J Biol Chem 284(5):2598–2602
81. Mbefo MK, Paleologou KE, Boucharaba A, Oueslati A, Schell H, Fournier M et al (2010) Phosphorylation of synucleins by members of the Polo-like kinase family. J Biol Chem 285(4):2807–2822
82. Goldberg AL (2003) Protein degradation and protection against misfolded or damaged proteins. Nature 426(6968):895–899
83. Klionsky DJ (2007) Autophagy: from phenomenology to molecular understanding in less than a decade. Nat Rev Mol Cell Biol 8(11):931–937
84. Vakifahmetoglu-Norberg H, Xia H, Yuan J (2015) Pharmacologic agents targeting autophagy. J Clin Invest. 125(1):5–13
85. Oueslati A, Schneider BL, Aebischer P, Lashuel HA (2013) Polo-like kinase 2 regulates selective autophagic α-synuclein clearance and suppresses its toxicity in vivo. Proc Natl Acad Sci U S A 110(41):E3945-3954
86. Achermann JC, Schwabe J, Fairall L, Chatterjee K (2017) Genetic disorders of nuclear receptors. J Clin Invest 127(4):1181–1192
87. Santos R, Ursu O, Gaulton A, Bento AP, Donadi RS, Bologa CG et al (2017) A comprehensive map of molecular drug targets. Nat Rev Drug Discov 16(1):19–34
88. Miyazaki M, Dobrzyn A, Elias PM, Ntambi JM (2005) Stearoyl-CoA desaturase-2 gene expression is required for lipid synthesis during early skin and liver development. Proc Natl Acad Sci USA 102(35):12501–12506
89. Mejhert N, Kuruvilla L, Gabriel KR, Elliott SD, Guie MA, Wang H et al (2020) Partitioning of MLX-family transcription factors to lipid droplets regulates metabolic gene expression. Mol Cell 77(6):1251-1264.e9
90. Witting LA, Horwitt MK (1964) Effect of degree of fatty acid unsaturation in tocopherol deficiency-induced creatinuria. J Nutr 82:19–33
91. Ramalingam N, Jin SX, Moors TE, Fonseca-Ornelas L, Shimanaka K, Lei S et al (2023) Dynamic physiological α-synuclein S129 phosphorylation is driven by neuronal activity. NPJ Park Dis 9(1):4
92. Sancenon V, Lee SA, Patrick C, Griffith J, Paulino A, Outeiro TF et al (2012) Suppression of α-synuclein toxicity and vesicle trafficking defects by phosphorylation at S129 in yeast depends on genetic context. Hum Mol Genet 21(11):2432–2449
93. Gorbatyuk OS, Li S, Sullivan LF, Chen W, Kondrikova G, Manfredsson FP et al (2008) The phosphorylation state of Ser-129 in human alpha-synuclein determines neurodegeneration in a rat model of Parkinson disease. Proc Natl Acad Sci USA 105(2):763–768
94. Tenreiro S, Reimão-Pinto MM, Antas P, Rino J, Wawrzycka D, Macedo D et al (2014) Phosphorylation modulates clearance of alpha-synuclein inclusions in a yeast model of Parkinson's disease. PLoS Genet 10(5):e1004302
95. Liu Y, Wang P, Jin G, Shi P, Zhao Y, Guo J et al (2023) The novel function of bexarotene for neurological diseases. Ageing Res Rev 90:102021
96. Volakakis N, Tiklova K, Decressac M, Papathanou M, Mattsson B, Gillberg L et al (2015) Nurr1 and retinoid X receptor ligands stimulate ret signaling in dopamine neurons and can alleviate α-synuclein disrupted gene expression. J Neurosci Off J Soc Neurosci 35(42):14370–14385